Influence of Alkylene Spacer Length on Thermal Enhancement of Photoinduced Optical Anisotropy in Photo-Cross-Linkable Liquid Crystalline Polymeric Films and Their Composites with Non-Liquid-Crystalline Monomers

Nobuhiro Kawatsuki,*,† Ryoji Tsutsumi,† Hirofumi Takatsuka,‡ and Takeya Sakai‡

Department of Materials Science and Chemistry, Himeji Institute of Technology, University of Hyogo, 2167 Shosha Himeji, 671-2201 Japan, and Hayashi Telempu Co. Ltd., 100-2 Machiyabora, Kamekubi, Toyota, 470-0375 Japan

Received May 10, 2007; Revised Manuscript Received June 10, 2007

ABSTRACT: Thermally enhanced photoinduced reorientation in a photo-cross-linkable liquid crystalline polymethacrylate comprised of 4-(*ω*-cinnamoyloxyalkyloxy)biphenyl side groups is investigated by irradiating with linearly polarized ultraviolet (LPUV) light and subsequent annealing at elevated temperatures. An odd−even effect of the alkylene spacer length between the cinnamate end group and biphenyl group on the transition temperatures of the polymer, photoinduced optical anisotropy, and thermal amplification of the in-plane molecular reorientation of thin films are observed. Because of the higher straight-line characteristics of the mesogenic side groups with an odd number alkylene spacer, the axis-selectivity of the anisotropic photoreaction of the photoreactive groups is greater than that with an even number, which leads to a larger photoinduced optical anisotropy and effective molecular reorientation. Finally, the cooperative reorientation in composites of the polymer and nonliquid crystalline monomer is explored to amplify the reorientational order of the film. The resultant reoriented composite film exhibits an in-plane order parameter of 0.52 and birefringence at 633 nm of 0.15.

1. Introduction

Photocontrol of the molecular orientation in a polymeric film is a promising technique applicable to birefringent optical devices, the photoalignment layer of liquid crystal displays, optical memories, and holographic data storage devices.[1−7] When a photoreactive polymeric film is exposed to linearly polarized (LP) light, a small optical anisotropy is created based on a polarization-axis selective photoreaction.[1−9] However, the photoinduced optical anisotropy in a photoreactive polymeric film is generally insufficient for birefringent optical device applications.[8] Therefore, an axis-selective photoreaction should be accompanied by a molecular reorientation to derive a large optical anisotropy. As materials that generate a large photoinduced optical anisotropy, various types of photoreactive polymers, which contain azobenzene groups and photo-cross-linkable groups, have been investigated.[9−14] Adjusting the polarization of the writing LP light beams leads to a reversible photoinduced optical anisotropy in azobenzene-containing polymeric films based on an axis-selective *trans*−*cis*−*trans* photoisomerization.[15] However, azobenzene-containing polymeric films are not suitable for display applications because the azobenzene moiety is colored in the visible region. Alternatively, axis-selective photo-cross-linking in polymeric films comprised of cinnamate derivatives, which are transparent in the visible region, only generates a small optical anisotropy upon irradiating with LP ultraviolet (LPUV) light.[8,13,14] However, a thermally enhanced self-organization to induce a molecular reorientation occurs when a material exhibits a liquid crystalline (LC) nature.[13,14]

We have carried out systematic studies on the photoinduced molecular reorientation in photo-cross-linkable polymer LC (PPLC) films containing mesogenic side groups terminated with cinnamate derivatives.[13,14,16−18] Irradiating these PPLC films with LPUV light generates a small photoinduced optical anisotropy, and a subsequent thermal treatment enhances the molecular reorientation due to the LC nature of the material. The axis-selective photoreacted groups act as a photo-cross-linked anchor that thermally reorients the non-photoreacted mesogenic groups parallel to the polarization (**E**) of LPUV light.[13,14] These reoriented films are applicable to passive optical devices such as birefringent films for liquid crystal displays and polarization holographic gratings.[5] Among them, it has been demonstrated that polymethacrylates with 4-cinnamoyloxybiphenyl (CB) side groups (Figure 1a) exhibit efficient in-plane molecular reorientations.[14] In contrast, when an ethylene spacer is introduced between the cinnamate end groups and biphenyl moiety [4-(2-cinnamoyloxy-ethoxy)biphenyl (CEB) side group, Figure 1b], the thermally enhanced in-plane molecular reorientation is small with an in-plane order parameter less than 0.05.[13c,d] This indicates that the ethylene spacer between the cinnamate end groups and the biphenyl moiety affects the axis-selectivity of the photoreaction of the cinnamoyl groups and the thermal enhancement of the photoinduced optical anisotropy of the film.

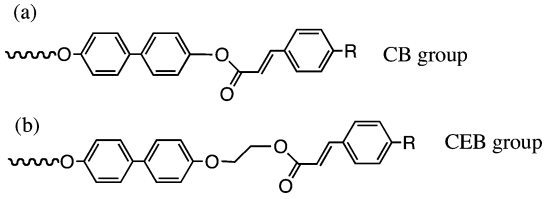

Figure 1. Photoreactive side groups used in PPLCs.

Additionally, copolymers, which are comprised of a photoreactive mesogenic side group and a photoinactive mesogenic group, have been investigated to generate cooperative molecular reorientation with a relatively higher in-plane order.[19−23]

* To whom correspondence should be addressed. E-mail: kawatuki@eng.u-hyogo.ac.jp. Telephone: +81-792-67-4886. Fax: +81-792-66-4885.
† Department of Materials Science and Chemistry, Himeji Institute of Technology, University of Hyogo.
‡ Hayashi Telempu Co. Ltd..

10.1021/ma071061l CCC: $37.00
Published on Web 07/18/2007

Scheme 1

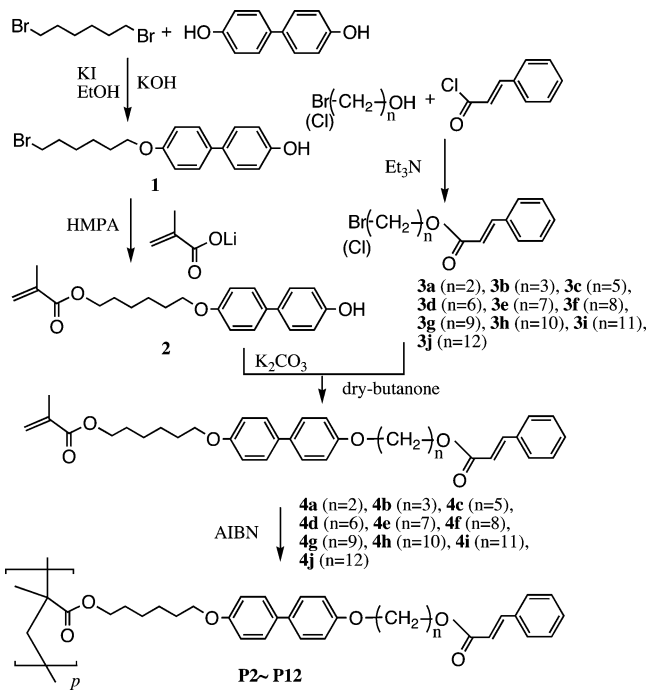

A methacrylate copolymer comprised of CEB side groups and 4-cyanobiphenyl side groups displays a thermally enhanced in-plane order of 0.4 when the exposed film is annealed in the LC temperature range of the material.[19] Cooperative reorientation of copolymer methacrylate films comprised of 4-subsutituted CEB side groups[13d] and light-emissive side groups has also been reported.[22] Furthermore, doping monomeric materials containing a biphenyl moiety with a homopolymer comprised of CEB side groups exhibit larger cooperative molecular reorientations.[23] In these cases, the axis-selectivity of the photoreaction of the photoreactive mesogenic groups influences the cooperative reorientation of the copolymer film.

It is expected that adjusting the alkylene spacer length between the cinnamoyl end group and the biphenyl group of the PPLC film containing the CEB derivatives will alter the photoinduced optical anisotropy and thermal enhancement of the in-plane molecular reorientation. However, the influence of the alkylene spacer length on the thermally enhanced photoinduced optical anisotropy in homopolymer LCs that contain CEB derivatives has yet to be explored. In this paper, photo-crosslinkable liquid crystalline polymethacrylates comprised of 4-(ω-cinnamoyloxy−alkyloxy)biphenyl side groups with various alkylene spacer lengths are synthesized to clarify the influence of the alkylene spacer length on the thermal property, photoinduced optical anisotropy, thermal enhancement of the molecular reorientation, and optical property of a reoriented film. In all cases, exposing the thin films to LPUV light generates a small optical anisotropy and thermal enhancement, but an odd−even effect of the alkylene spacer length is revealed. Finally, cooperative photoinduced molecular reorientation in composites of the polymer and non-liquid-crystalline monomer is evaluated to achieve a larger in-plane reorientation.

2. Experimental Section

2.1. Materials. All starting materials were used as received from Tokyo Kasei Chemicals. Monomers and polymers were synthesized according the procedure shown in Scheme 1.

4-(6-Bromohexyloxy)-4′-hydroxybiphenyl (1). To a solution of 50 g (0.27 mol) 4−4′-biphenol, 18 g (0.32 mol) potassium hydroxide and a small amount of KI in 400 mL of ethanol was added 53 g (0.22 mol) of dibromohexane, and the reaction was refluxed for 20 h. After filtration and washing with ethyl acetate, the solution was evaporated, and the resultant solid was washed with a dilute NaOH solution and water. The crude products were recrystallized from ethanol/ethyl acetate. Yield: 7.8 g (0.022 mol, 10%). Mp = 125−130 °C. ^{1}H NMR ($CDCl_3$) δ (ppm) = 1.50−1.54 (m, 4H), 1.80−1.84 (m, 2H), 1.88−1.93 (m, 2H), 3.42 (t, 2H, J = 6.8 Hz), 3.98 (t, 2H, J = 6.3 Hz), 6.88 (d, 2H, J = 8.3 Hz), 6.92 (d, J = 8.3 Hz), 7.40 (d, 2H, J = 8.3 Hz), 7.43 (d, J = 8.3 Hz).

Table 1. Yield, Molecular Weight, and Thermal Properties of the Synthesized Polymers

			mol wt (g/mol)[a]		
polymer	n	yield (%)	$M_n \times 10^{-4}$	M_w/M_n	transition temp (°C)[b]
P2	2	53	2.5	2.1	G 40 N 74 I
P3	3	63	4.6	2.6	G 110 N 136 I
P5	5	60	6.4	2.1	G 85 N 125 I
P6	6	55	4.6	2.5	G 57 N 117 I
P7	7	16	2.8	1.6	G 91 N 130 I
P8	8	60	5.1	2.2	G 75 N 121 I
P9	9	62	6.3	3.8	G 115 N 124 I
P10	10	41	2.9	1.7	G 81 N 125 I
P11	11	50	4.2	2.1	G 97 N 123 I
P12	12	40	2.5	1.8	G 90 N 125 I

[a] Measured by GPC, polystyrene standards. [b] Determined by DSC.

4-(6-Methacryloxyhexyloxy)-4′-hydroxybiphenyl (2). To a solution of 7.2 g (0.021 mol) of **1** in 70 mL of hexamethylphosphoric triamide (HMPA) was added 1.5 g (0.017 mol) lithium methacrylate, and the reaction was stirred at 40 °C for 60 h. The solution was poured into 2.5 L of water. The precipitate was filtered and dried under reduced pressure. Yield: 4.3 g (0.012 mol, 72%). Mp = 56−58 °C. ^{1}H NMR ($CDCl_3$) δ (ppm) = 1.50−1.54 (m, 4H), 1.75−1.84 (m, 4H), 1.99 (s, 3H), 3.98 (t, 2H, J = 6.8 Hz), 4.85 (t, 2H, J = 6.5 Hz), 5.58 (s, 1H), 6.10 (s, 1H), 6.85 (d, 2H, J = 7.8 Hz), 6.92 (d, J = 7.8 Hz), 7.40 (d, 2H, J = 7.9 Hz), 7.44 (d, J = 7.8 Hz).

6-Bromoheptyl Cinnamate (3e). To a solution of 6.4 g (0.032 mol) of 7-bromo-1-heptanol and 5.0 g (0.050 mol) of triethyl amine in 50 mL of chloroform was added 6.8 g (0.041 mol) of cinnamoyl chloride in 70 mL of chloroform, and the reaction was stirred at room temperature for 24 h. Then the reaction mixture was poured into 100 mL of water, and extracted with chloroform three times. The chloroform solution was dried over Na_2SO_4 and evaporated under a reduced pressure. The crude product was purified by silica-gel chromatography (eluent: chloroform). Yield: 9.6 g (0.029 mol, 92%) of a viscous liquid. ^{1}H NMR ($CDCl_3$) δ (ppm) = 1.35−1.49 (m, 6H), 1.70−1.89 (m, 4H), 3.42 (t, 2H, J = 6.8 Hz), 4.21 (t, 2H, J = 6.8 Hz), 6.45 (d, 1H, J = 5.9 Hz), 7.40 (d, 2H, J = 3.6 Hz), 7.53 (d, 2H, J = 3.6 Hz), 7.69 (d, 1H, J = 5.9 Hz).

Other compounds (**3a**−**3d** and **3f**−**3j**) were synthesized according to similar methods using ω-bromo- (or chloro-) alkyl-1-ol. All compounds were viscous liquids and were confirmed by ^{1}H NMR. Yields were between 87 and 95%.

4-(6-Methacryloxyhexyloxy)-4′-(6-cinnamoyloxyheptyloxy)biphenyl (4e). To a solution of 5.0 g (0.014 mol) of **2**, 12.0 g (0.086 mol) of potassium carbonate, and 10 mg of 2,6-di-*tert*-butyl-4-methylphenol (inhibitor) in 50 mL of dry butanone was added 5.4 g (0.016 mol) of **3e** in 50 mL of dry-butanone, and the reaction was stirred under reflux for 24 h. After filtration and washing with butanone, the solution was evaporated. The crude products were recrystallized from ethanol/ethyl acetate. Yield: 2.3 g (0.0039 mol, 27%). Mp = 73−75 °C. ^{1}H NMR ($CDCl_3$) δ (ppm) = 1.41−1.52 (m, 10H), 1.71−1.77 (m, 4H), 1.80−1.86 (m, 4H), 1.95 (s, 3H), 3.99 (t, 4H, J = 6.4 Hz), 4.16 (t, 2H, J = 6.6 Hz), 4.21 (t, 2H, J = 6.6 Hz), 5.54 (s, 1H), 6.10 (s, 1H), 6.45 (d, 1H, J = 5.9 Hz), 6.93−6.95 (m, 4H), 7.40−7.62 (m, 9H), 7.68 (d, 1H, 5.9 Hz).

Other methacrylate monomers (**4a**−**4d**, and **4f**−**4j**) were synthesized according to similar methods using **2** and the corresponding

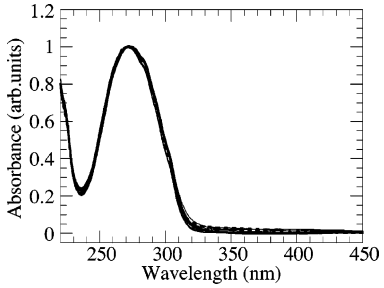

Figure 2. Absorption spectra of the synthesized polymer films on quartz substrates.

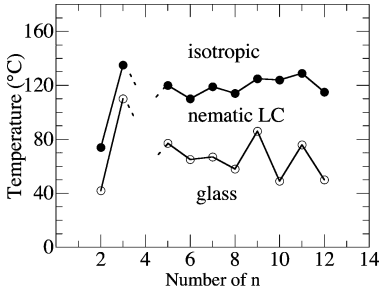

Figure 3. Transition temperatures of polymers with different alkylene spacer lengths.

3a−**3j** and were confirmed by ^{1}H NMR. Yields were between 10 − 27%. Mp = 82−83 (**4a**), 79−80 (**4b**), 78−81 (**4c**), 69−70 (**4d**), 79−82 (**4f**), 74−76 (**4g**), 90−92 (**4h**), 81−83 (**4i**), and 72−73 °C (**4j**).

2.2. Polymer Synthesis. Polymers **P2**−**P12** were synthesized from corresponding monomers **4a**−**4j** by a free radical solution polymerization in THF at 57 °C for 1 day. Monomer and AIBN concentrations were 10% w/v and 2 mol %, respectively. After the reaction, a polymer was obtained by adding the homogeneous solution into excess diethyl ether. The polymer was further purified by precipitation twice from a dichloromethane solution into diethyl ether. All synthesized polymers were confirmed by ^{1}H NMR. Table 1 summarizes the molecular weights and thermal properties of the synthesized polymers.

2.3. Photoreaction. Thin polymer films, which were approximately 0.2−0.3 μm thick, were prepared by spin-coating a chloroform solution of polymers (1−2% w/w) onto quartz or KBr substrates. LPUV light, which had an intensity of 150 mW cm^{-2} at 365 nm produced by using an ultrahigh-pressure Hg lamp equipped with Glan-Taylor polarizing prisms and a cutoff filter under 290 nm, was used in the photoreactions. The conversion for the photoreaction of the film was estimated using UV spectroscopy to monitor the decrease in absorbance at 272 nm (λ_{max}).

2.4. Characterization. The monomers and polymers were confirmed by the ^{1}H NMR spectra with a Bruker DRX-500 FT-NMR and FTIR spectra (JASCO FTIR-410). A GPC (Tosoh HLC-8020 GPC system with Tosoh TSKgel column; eluent, chloroform), which was calibrated using polystyrene standards, was used to measure the molecular weight of the polymers. The thermal properties were examined using a polarization optical microscope (POM; Olympus BX51) equipped with a Linkam TH600PM heating and cooling stage in addition to differential scanning calorimetry (DSC; Seiko-I SSC5200H) analysis at a heating and cooling rate of 10 °C min^{-1}. The polarization absorption spectra were measured with a Hitachi U-3010 spectrometer equipped with Glan-Taylor polarization prisms.

The photoinduced optical anisotropy, ΔA, which is expressed as eq 1, was evaluated using the polarization absorption spectra,

$$\Delta A = A_{\parallel} - A_{\perp} \tag{1}$$

where $A_{\parallel}$ and $A_{\perp}$ are the absorbances parallel and perpendicular to **E**, respectively. To enhance the molecular reorientation, the thin films were annealed after photoirradiation at a temperature close to the T_i of the polymer for 10 min. The thermally enhanced in-plane order, S, is expressed as eq 2.

$$S = \frac{A_{\parallel\prime} - A_{\perp}}{A_{//} + 2A_{\perp}} \tag{2}$$

The birefringence (Δn) of a reoriented film was measured by the Senarmont method at 633 nm.

3. Results and Discussion

3.1. Spectroscopic and Thermal Property of PPLCs. As shown in Figure 2, all the synthesized polymers exhibit similar absorption spectra. Because the absorption bands of the biphenyl moiety (λ_{max} = 265 nm) and that of cinnamate moiety (λ_{max} = 275 nm) are close to each other, the absorption spectrum reveals a monomodal curve. All the polymers exhibit a nematic LC nature (Table 1). Figure 3 plots the transition temperature vs alkylene spacer length, which shows an odd−even effect. The influence of the alkylene spacer length is large for **P2** and **P3**, indicating a large difference in the conformation of the mesogenic side groups between these polymers. The odd−even effect of the alkylene group lengths on the transition temperature is due to conformational differences of the mesogenic side groups in the solid and LC states, which is typical of LC monomers and polymers.[24]

3.2. Axis-Selective Photoreaction. Irradiating with LPUV light causes an axis-selective photoreaction in polymeric films comprised of cinnamate derivatives, which generates a negative optical anisotropy (ΔA) in the film.[3,8,25] Parts a and b of Figure 4 plot the conversion, which is calculated by the change in the absorption intensity at 272 nm, and the photoinduced ΔA of the films as functions of the exposure energy of LPUV light, respectively. The films exhibit similar photoreactivities. Besides the photoreaction of the cinnamate groups, photodegradation of the biphenyl moiety and ester groups in methacrylate and cinnamate moiety is also detected, which is confirmed by the FT-IR spectroscopy (see the Supporting Information). This photodegradation occurs when the exposure energy is greater than 50 J cm^{-2}, which is an energy where most of the cinnamate groups have photoreacted.

The axis-selective photoreaction of the mesogenic groups generates a negative ΔA as shown in Figure 4b. The absolute negative ΔA values reach maxima (∼0.03) when the exposure energy is approximately 0.5−5 J cm^{-2} and the conversion is around 15−40%. However, the ΔA values decrease upon further irradiating. This small photoinduced ΔA in the early stage of photoexposure is mainly due to the axis-selective photoreaction of the cinnamate end groups. The decrease in ΔA around 20 J cm^{-2} doses is due to the saturation of the photoreaction of the cinnamate groups. When the exposure energy is greater than 50 J cm^{-2}, the absolute ΔA values again increases where the absolute ΔA values are near 0.08. As confirmed by the UV-absorption and FT-IR spectra, this increase is due to the axis-selective photodegradation of the biphenyl moieties. Additionally, Figure 5 plots the maximum photoinduced ΔA values when the conversion is around 15−40% and indicates an odd−even effect. This means that the axis-selectivity of the photoreaction of the mesogenic side groups is higher for polymers with an odd number of alkylene side groups than those with an even number.

3.3. Thermal Enhancement of the Photoinduced Optical Anisotropy. We have reported that the photoinduced negative optical anisotropy of a **P2** film is reversely amplified when the exposed film is annealed at a temperature near Ti of the

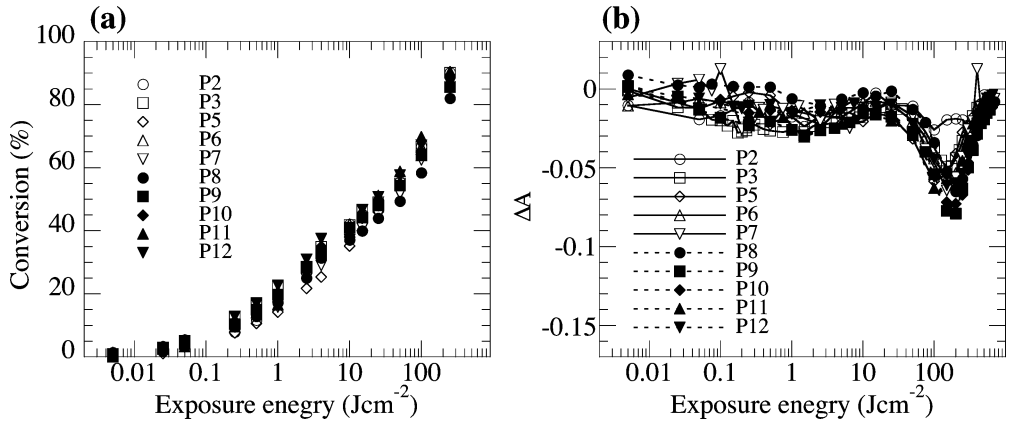

Figure 4. (a) Conversion of polymer films and (b) photoinduced optical anisotropy ($\Delta A = A_{\parallel} - A_{\perp}$) of the polymer films as functions of exposure energy.

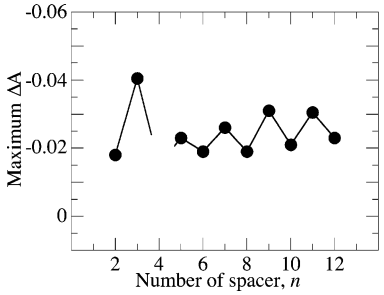

Figure 5. Maximum photoinduced ΔA values in the early stage of the photoreaction for polymer films with different alkylene spacer lengths.

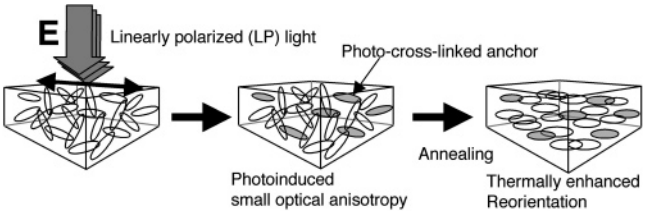

Figure 6. Illustration of the thermally enhanced photoinduced molecular reorientation of a PPLC film.

polymer.[13c,26] Figure 6 illustrates the mechanism of the thermally enhanced molecular reorientation of PPLC films parallel to the polarization **E** of exposed LPUV light. This thermally enhanced molecular reorientation is due to the axis-selective photoreacted groups, which act as a photo-cross-linked anchor and thermally reorient the unphotoreacted mesogenic groups along them.[13,14,26] However, the generated in-plane orientational order (S) of the **P2** film is less than 0.05, and the induced birefringence (Δn) is less than 0.02.[13c] Because the conformation between the cinnamate and biphenyl groups of the mesogenic side groups should depend on the length of the alkylene spacer, its conformation affects the axis-selectivity of the photoreaction of the side groups and thermally enhanced S values.

Parts a and b of Figure 7 show changes in the polarization UV−vis absorption spectra of the **P2** and **P3** films irradiated with LPUV light and the spectra after subsequent annealing at a temperature close to Ti of the polymer for 10 min, respectively. The insets are magnified views. The conversion is approximately 12 mol % for both films and in both cases, irradiating with LPUV light induces a small negative optical anisotropy, while subsequent annealing reversely generates the molecular reorientation parallel to **E**. The amplified S value of the **P3** film is 0.27, which is much greater than that of **P2** ($S = 0.04$). Additionally, the inset of Figure 7 reveals that the photoinduced

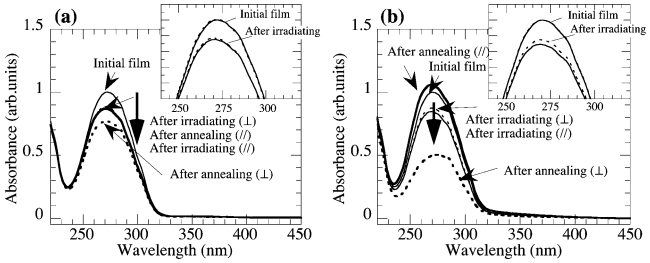

Figure 7. UV−vis polarization spectra of polymer films before photoirradiation, after irradiation (thin lines), and after subsequent annealing (thick lines) for 10 min. $A_{\parallel}$ is the solid lines, while $A_{\perp}$ is the dotted lines. Key: (a) **P2** film, annealing temperature 74 °C; (b) **P3** film, annealing temperature 125 °C. Inset is a magnified view.

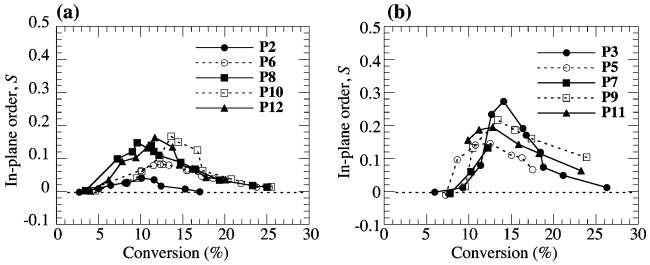

Figure 8. Thermally enhanced in-plane order, S, as a function of the conversion of the film. Annealing temperature: **P2** = 74, **P3** = 125, **P5** = 123, **P6** = 120, **P7** = 129, **P8** = 120, **P9** = 125, **P10** = 124, **P11** = 129, and **P12** = 115 °C. Key: (a) even number alkylene spacer; (b) odd number alkylene spacer.

ΔA of the **P3** film ($\Delta A = -0.031$) is larger than that of **P2** ($\Delta A = -0.008$). These results suggest that a larger photoinduced ΔA leads to a greater thermally enhanced molecular reorientation of the film.

Other polymer films exhibit similar phenomena. Parts a and b of Figure 8 plot the thermally enhanced S values of the polymer films with even and odd number alkylene spacers, respectively, as a function of conversion. The annealing temperature is near Ti for all cases. Maximum S values are obtained when the conversion is around 10−18%, and the enhanced S values of films with an odd number alkylene spacer are larger than that with an even number. Figure 9 plots the maximum S values and the photoinduced ΔA values for each polymer films with different alkylene spacer lengths. Both the photoinduced ΔA and thermally enhanced S values with an odd number alkylene spacer are larger than that with even ones. The influence of the alkylene spacer length is remarkable for polymers with short alkylene spacers, where the ΔA and S values are much larger for **P3** and much smaller for **P2**. These results

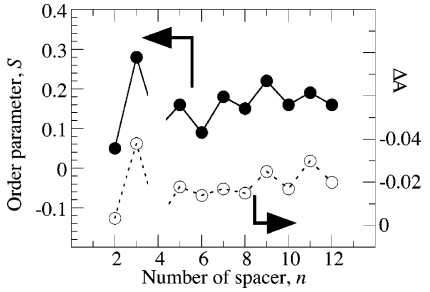

Figure 9. Maximum in-plane order, *S*, and photoinduced Δ*A* values or polymer films with different alkylene spacer lengths.

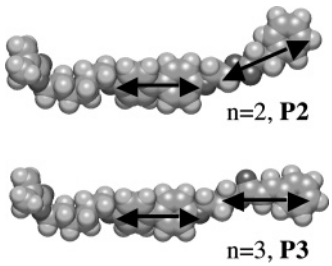

Figure 10. Stable molecular structures of the mesogenic side groups of **P2** and **P3** calculated by MOPAC.

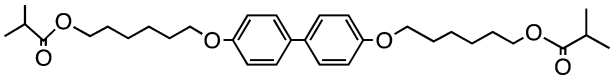

Figure 11. Chemical structure of doped monomer **M6B**.

indicate that the conformation of the mesogenic groups in a solid film depends on the alkylene spacer length, and the difference in the conformation is large when the alkylene spacer length is short.

This odd−even effect is due to the difference in the conformation of the mesogenic side groups. Figure 10 shows the stable molecular structure of the mesogenic side groups of **P2** and **P3** calculated by a semiempirical molecular orbital method (MOPAC). The MOPAC results indicate that the angle between the biphenyl group and the cinnamate groups of **P2** is larger than that of **P3**. This difference in the conformation of the mesogenic side groups leads to a lower polarization axis-selectivity of the photoreaction for **P2** compared to that for **P3** because the straight line of the mesogenic groups of **P2** is lower than that of **P3**. Because the absorption bands of the biphenyl and cinnamate groups are close to each other, photoabsorption of the biphenyl groups will deteriorate the axis-selection of the photoreaction of the cinnamate groups when these groups are not in the straight line. Namely, the straight-line characteristics between the biphenyl mesogenic core and photoreactive cinnamate moiety play an important role in the axis-selectivity of the polarization-selective photoreaction of the mesogenic side groups.

3.4. Amplification of the in-Plane Reorientation Order by Doping with a Rodlike Monomer. We have reported a cooperative molecular reorientation of a **P2** film doped with a non-LC rodlike monomer, **M6B** (Figure 11), by irradiating with LPUV light and subsequent annealing.[23] Because the in-plane *S* values are larger than that for a **P2** film without **M6B**, the reoriented film may be applicable to a birefringent film for liquid crystal displays (LCDs).[23a] The axis-selective photoreacted anchor parallel to **E** reorients **M6B**, which results in a cooperative molecular reorientation of the mesogenic side groups of **P2**. In this section, the influence of the alkylene spacer length on this cooperative reorientation using **P2** and **P3** doped with **M6B** is described.

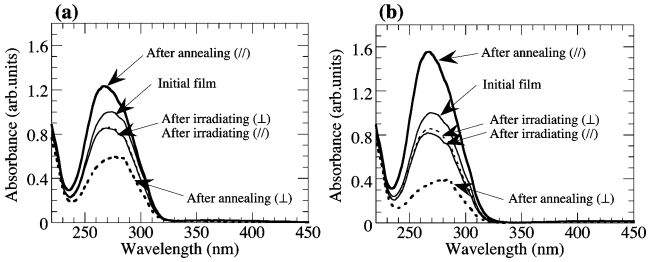

Figure 12. UV−vis polarization spectra of polymer/**M6B** composite films before photoirradiation, after irradiation (thin lines), and after subsequent annealing (thick lines) for 10 min. $A_{\parallel}$ is the solid lines, while $A_{\perp}$ is the dotted lines. Content of **M6B** is 25 wt %. Key: (a) **P2**/**M6B** film, annealing temperature 80 °C; (b) **P3**/**M6B** film, annealing temperature 110 °C.

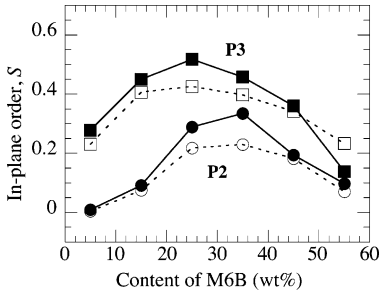

Figure 13. Maximum in-plane order, *S*, for polymer/**M6B** composite films with different **M6B** content. Closed points are *S* values of the polymer/**M6B** composite films, and open points are the *S* values after extracting **M6B**.

Table 2. Thermal Property of Polymer/M6B Composites

polymer	M6B content (wt %)	transition temp (°C)[a]
none	100	C 58 I
P2	5	G 35 N 55 I
P2	25	G 40 I
P2	45	G 38 I
P3	5	G 107 N 132 I
P3	25	G 102 N 125 I
P3	45	G 102 N 112 I

[a] Determined by DSC and POM observation.

Table 2 summarizes the thermal property of polymer/**M6B** composites. All the composite films are transparent, and POM observation does not show clear liquid crystalline texture for the **P2**/**M6B** composites when the content of **M6B** is high,[23] while decrease in the transition temperatures is observed for **P3**/**M6B** composites. This means that **M6B** is dissolved in the **P2** or **P3** matrix and acts as a plasticizer in the composite film. Parts a and b of Figure 12 compare the changes in the polarization UV−vis absorption spectra of the **P2** and **P3** films doped with 25 wt % of **M6B** irradiated with LPUV light and after subsequent annealing at 80 °C for **P2/M6B** and 110 °C for **P3/M6B**, for 10 min, respectively. The conversion is approximately 15% for both composite films. The enhanced *S* values are 0.26 for **P2/M6B** and 0.52 for **P3/M6B**, and the generated birefringence (Δ*n*) values are 0.10 for **P2/M6B** and 0.15 for **P3/M6B**. These values are much larger than those for films without **M6B**, indicating a cooperative reorientation of the mesogenic side groups and **M6B**. Furthermore, the enhanced *S* and Δ*n* values of **P3/M6B** are larger than that of **P2/M6B** because the absolute value of the photoinduced Δ*A* for **P3/M6B** composite ($\Delta A = -0.039$) is larger than that for **P2/M6B** ($\Delta A = -0.008$). These results indicate that similar to the case of a polymer film without **M6B**, a cooperative molecular reorientation is effective when the photoinduced Δ*A* value is larger. The larger Δ*n* value makes the birefringent film thinner and lighter.

Figure 13 plots the influence of the **M6B** content on the thermally enhanced *S* values along with the *S* values after extracting **M6B** by immersing the reoriented film in diethyl ether. For both polymers, a maximum *S* value is obtained when the content of **M6B** is 15 − 35 wt %. The larger *S* values for the **P3/M6B** composite is due to the higher axis-selectivity of the photoreaction of the mesogenic side groups of **P3**. Additionally, the *S* values after the extraction of **M6B** are maintained for both composite films, indicating that the reorientational orders of both mesogenic groups of the polymer and **M6B** are similar.

4. Conclusion

Photo-cross-linkable liquid crystalline polymethacrylates comprised of 4-(ω-cinnamoyloxy−alkyloxy)biphenyl side groups were synthesized. The axis-selective photoreaction of their thin films using LPUV light was explored in order to investigate the influence of the alkylene spacer length on the photoinduced optical anisotropy and the thermally enhanced molecular reorientation behavior. The straight-line characteristic of the mesogenic side groups played an important role in the generation of a larger photoinduced optical anisotropy in the polymer film. Furthermore, a large photoinduced optical anisotropy led to a larger thermal enhancement of the molecular reorientation. Finally, the photoinduced reorientations in composite films of the polymer and non-liquid-crystalline monomer were investigated in order to improve the molecular reorientation when a cooperative molecular reorientation is observed. The resultant **P3/M6B** composite film exhibited a reorientational order of 0.52 and a generated birefringence of 0.15. This composite film may be applicable as a thin phase retarder for LCDs. Further investigations on the three-dimensional molecular orientation using a slantwise LPUV light exposure are underway.

Acknowledgment. This work was partly supported by Grant-in-Aid for Scientific Research (S, No.16105004 and B, No. 17350111) by Japan Society for the Promotion of Science.

Supporting Information Available: Figure showing change in UV absorption and FT-IR spectrum of P2 film. This material is available free of charge via the Internet at http://pubs.acs.org.

References and Notes

(1) (a) Shibaev, V. P.; Kostromin, S. G.; Ivanov, S. A. *Polymers as Electroactive and Photooptical Media*; Shibaev, V. P., Ed.; Springer: Berlin, 1996; pp 37−110. (b) MacArdle, C. B. *Applied Photochromic Polymer Systems*; MacArdle, C. B. Ed.; Blackie: New York, 1991; pp 1−30. (c) Krongauz, V. *Applied Photochromic Polymer Systems*,; MacArdle, C. B. Ed.; Blackie: New York, 1991; pp 121−173.

(2) Anderle, K.; Birenheide, R.; Eich, M.; Wendrorff, J. H. *Makromol. Chem. Rapid. Commun.* **1989**, *10*, 477−483.

(3) (a) Schadt, M.; Schmitt, K.; Kozinkov, V.; Chigrinov, V. *Jpn. J. Appl. Phys.* **1992**, *31*, 2155−2164. (b) O'Neill, M.; Kelly, S. M. *J. Phys. D: Appl. Phys.* **2000**, *33*, R67−R84. (c) Schadt, M.; Seiberle, H.; Schuster, A. *Nature* **1994**, *381*, 212−215.

(4) (a) Fischer, T.; Läsker, L.; Czapla, S.; Rübner, J.; Stumpe, J. *Mol. Cryst. Liq. Cryst.* **1997**, *298*, 213−220. (b) Rutloh, M.; Stumpe, J.; Stachanov, L.; Kostromin, S.; Shibaev, V. *Mol. Cryst. Liq. Cryst.* **2000**, *352*, 149−157.

(5) (a) Kawatsuki, N.; Kawakami, T.; Yamamoto, T. *Adv. Mater.* **2001**, *13*, 1337−1339. (b) Kawatsuki, N.; Hasegawa, T.; Ono, H.; Tamoto, T. *Adv. Mater.* **2003**, *15*, 991−994.

(6) Häckel, M.; Kador, L.; Kropp, D.; Schmidt, H.-W. *Adv. Mater.* **2007**, *19*, 227−231.

(7) (a) Ikeda, T.; Tsutsumi, O. *Science* **1995**, *268*, 1873−1875. (b) Saishoji, A.; Sato, D.; Shishido, A.; Ikeda, T. *Langmuir* **2007**, *23*, 320−326. (c) Ishiguro, M.; Sato, D.; Shishido, A.; Ikeda, T. *Langmuir* **2007**, *23*, 32−338.

(8) Barachevsky, V. A. *Proc. SPIE* **1991**, *1559*, 184−193.

(9) (a) Ichimura, K. *Chem. Rev.* **2000**, *100*, 1847−1873. (b) Natansohn, A.; Rochon, P. *Chem. Rev.* **2002**, *102*, 4139−4176. (c) Ikeda, T. *J. Mater. Chem.* **2003**, *13*, 2037−2057.

(10) (a) Kukinna, Ch.; Zebger, I.; Hvilsted, S.; Ramanujam, P. S.; Siesler, H. W. *Macromol. Symp.* **1994**, *83*, 169−181. (b) Kempe, C.; Rutloh, M.; Stumpe, J. *J. Phys.: Condens. Matter.* **2003**, *15*, S813−S823.

(11) (a) Wu, Y.; Demachi, Y.; Tsustusmi, O.; Kanazawa, A.; Hisono, T.; Ikeda. T. *Macromolecules* **1998**, *31*, 4457−4463. (b) Wu, Y.; Demachi, Y.; Tsustusmi, O.; Kanazawa, A.; Hisono, T.; Ikeda, T. *Macromolecules* **1998**, *31*, 1104−1108.

(12) Han, M.; Ichimura, K. *Macromolecules* **2001**, *34*, 82−89. (b) Han, M.; Ichimura, K. *Macromolecules* **2001**, *34*, 90−98. (c) Han, M.; Morino, S.; Ichimura, K. *Macromolecules* **2000**, *33*, 6360−6370.

(13) (a) Kawatsuki, N.; Sakashita, S.; Takatani, K.; Yamamoto, T.; Sangen, O. *Macromol. Chem. Phys.* **1996**, *197*, 1919−1935. (b) Kawatsuki, N.; Takatsuka, H.; Yamamoto, T.; Sangen, O. *Macromol. Rapid Commun.* **1996**, *17*, 703−712. (c) Kawatsuki, N.; Takatsuka, H.; Yamamoto, T.; Sangen, O. *J. Polym. Sci., Part A: Polym. Chem.* **1998**, *36*, 1521−1526. (d) Kawatsuki, N.; Kawakami, K.; Arita, T.; Yamamoto, T. *Kobunshi Ronbunshu* **1999**, *56*, 234−239 (in Japanese).

(14) Kawatsuki, N.; Goto, K.; Kawakami, T.; Yamamoto, T. *Macromolecules* **2002**, *35*, 706−713.

(15) Shi, Y.; Steier, W. H.; Yu, L.; Chen, M.; Dalton, L. R. *Appl. Phys. Lett.* **1991**, *59*, 2935−2937.

(16) Kawatsuki, N.; Ono, H.; Takatsuka, H.; Yamamoto, T.; Sangen, O. *Macromolecules* **1997**, *30*, 6680−6682.

(17) (a) Kawatsuki, N.; Tachibana, T.; An, M. X.; Kato, K. *Macromolecules* **2005**, *38*, 3903−3908. (b) Kawatsuki, N.; Kato, K.; Shiraku, T.; Ono, H. *Macromolecules* **2006**, *39*, 3245−3251.

(18) Uchida, E.; Kawatsuki, N. *Macromolecules* **2006**, *39*, 9357−9364.

(19) (a) Kawatsuki, N.; Suehiro, C.; Yamamoto, T. *Macromolecules* **1998**, *31*, 5984−5990. (b) Kawatsuki, N.; Matsuyoshi, K.; Yamamoto, T. *Macromolecules* **2000**, *33*, 1698−1702.

(20) Kawatsuki, N.; Furuso, N.; Goto, K.; Yamamoto, T. *Macromol. Chem. Phys.* **2002**, *203*, 265−270. (b) Kawatsuki, N.; Furuso Uchida, E.; Yamamoto, T. *Macromol. Chem. Phys.* **2002**, *203*, 2438−2445.

(21) (a) Läsker, L.; Fischer, T.; Stumpe, J.; Kostromin, S.; Ivanov, S.; Shibaev, V.; Ruhmann, R. *Mol. Cryst. Liq. Cryst.* **1994**, *293*, 1−10. (b) Fischer, T.; Läsker, L.; Stumpe, J.; Kostromin, S. *J. Photochem. Photobiol. A: Chem.* **1994**, *80*, 453−459. (c) Date, R. W.; Fawcett, A. H.; Geue, T.; Haferkorn, J.; Malcolm, R. K.; Stumpe, J. *Macromolecules* **1998**, *31*, 4935−4949.

(22) Rosenhauer, R.; Stumpe, J.; Giménez, R.; Piñol, M.; Serrano, J. L.; Viñuales, A. *Macromol. Rapid Commun.* **2007**, *28*, 932−936.

(23) (a) Kawatsuki, N.; Sakai, T.; An, M. X.; Hasegawa, T.; Yamamoto, T. *Proc. SPIE* **2001**, *4463*, 109−116. (c) Kawatsuki, N.; An, M. X.; Hasegawa, T.; Yamamoto, T.; Sakai, T. *Jpn. J. Appl. Phys.* **2002**, *41*, L198−L200.

(24) (a) Percec, V.; Pugh, C. *Polymers as Side Chain Liquid Crystal Polymers*; McArdle, C. B., Ed.; Blackie: New York, 1989; pp 30−105. (b) Imrie, C. T. *Liquid Crystals II*; Mingos, D. M. P., Ed.; Springer, Berlin, 1999; pp 149−192.

(25) (a) Akita, Y.; Akiyama, H.; Kudo, K.; Hayashi, Y.; Ichimura, K. *J. Photopolym. Sci. Technol.* **1995**, *8*, 75−78. (b) Ichimura, K.; Akita, Y.; Akiyama, H.; Kudo, K.; Hayashi, Y. *Macromolecules* **1997**, *30*, 903−911. (c) Obi, M.; Morino, S.; Ichimura, K. *Jpn. J. Appl. Phys.* **1999**, *38*, L145−L147.

(26) Kawatsuki, N.; Takatsuka, H.; Yamamoto, T.; Sangen, O. *Jpn. J. Appl. Phys.* **1997**, *36*, 6464−6469.

MA071061L